Physics Letters B 792 (2019) 335–339

Contents lists available at ScienceDirect

Physics Letters B

www.elsevier.com/locate/physletb

Continuing influence of shell effects at high-excitation energies

Cebo Ngwetsheni, José Nicolás Orce *

Department of Physics & Astronomy, University of the Western Cape, Bellville-7535, South Africa

ARTICLE INFO

Article history:
Received 30 November 2018
Received in revised form 15 February 2019
Accepted 11 March 2019
Available online 15 March 2019
Editor: V. Metag

Keywords:
Nuclear dipole polarizability
Quasi-continuum
Low-energy enhancement
Photon-strength function
Photo-absorption cross sections
Magic numbers

ABSTRACT

Empirical drops in ground-state nuclear polarizabilities indicate deviations from the effect of giant dipole resonances and may reveal the presence of shell effects in semi-magic nuclei with neutron magic numbers $N = 50$, 82 and 126. Similar drops of polarizability in the quasi-continuum of nuclei with, or close to, magic numbers $N = 28$, 50 and 82, could reflect the continuing influence of shell closures up to the nucleon separation energy. These findings open a new avenue to investigating magic numbers at high-excitation energies and strongly support recent large-scale shell-model calculations in the quasi-continuum region, which describe the origin of the low-energy enhancement of the photon strength function as induced paramagnetism. The nuclear-structure dependence of the photon-strength function asserts the generalized Brink-Axel hypothesis as more universal than originally expected.

The ability for a nucleus to be polarized is a fortiori driven by the dynamics of the isovector giant dipole resonance (GDR). That is, the inter-penetrating motion of proton and neutron fluids out of phase [1], which results from the symmetry energy in the Bethe-Weizsäcker semi-empirical mass formula [2,3], $a_{sym}(\rho_N - \rho_Z)^2/\rho_A$, acting as a restoring force [1,4]. Respectively, ρ_N and ρ_Z are the mass densities of the neutron and proton fluids, and ρ_A the sum of the separate densities. The GDR represents most of the absorption and emission of γ-ray photons by a nucleus and was the first quantum collective excitation ever discovered in mesoscopic systems [5]. The idea of *giant resonances* was soon borrowed by atomic, molecular and solid-state physics (see e.g. [6] and references therein); the GDR motion is akin to the plasmons in graphene, which enables strong confinement of electromagnetic energy at subwavelength scales [7].

Using the collective variable ρ_Z as the potential energy of the liquid drop, Migdal calculated the electric dipole polarizability, α_{E1}, for the ground state of nuclei to be directly proportional to the size of the nucleus [1],

$$\alpha_{E1} = \frac{e^2 R^2 A}{40 a_{sym}} = 2.25 \times 10^{-3} A^{5/3}\ \text{fm}^3, \tag{1}$$

where $a_{sym} = 23$ MeV is the symmetry energy parameter and $R = 1.2A^{1/3}$ fm the radius of the nucleus with $A = N + Z$. Alternatively, α_{E1} is well described by microscopic mean-field approaches using the random-phase approximation (RPA) with various effective interactions [8–10], and can be determined empirically with the use of second-order perturbation theory,

$$\alpha_{E1} = 2e^2 \sum_n \frac{\langle i \parallel \hat{E1} \parallel n\rangle\langle n \parallel \hat{E1} \parallel i\rangle}{E_\gamma} = \frac{\hbar c}{2\pi^2}\sigma_{-2}, \tag{2}$$

with $|i\rangle$ being the vector of the ground state connecting high-lying $|n\rangle$ states in the GDR region via $E1$ virtual excitations, and σ_{-2} the (-2) moment of the total photo-absorption cross section [11,12] defined as,

$$\sigma_{-2} := \int_0^{E_{\gamma max}} \frac{\sigma_{total}(E_\gamma)}{E_\gamma^2}\, dE_\gamma, \tag{3}$$

where the total photonuclear-absorption cross section, $\sigma_{total}(E_\gamma)$, generally includes all $\sigma(\gamma, n)$ and $\sigma(\gamma, p)$ contributions [13].

Naturally, total σ_{-2} values should include both electric and magnetic polarizability contributions,

$$\sigma_{-2} = \frac{2\pi^2}{\hbar c}(\alpha_{E1} + \chi_{M1}), \tag{4}$$

* Corresponding author.
E-mail address: jnorce@uwc.ac.za (J.N. Orce).
URL: https://nuclear.uwc.ac.za (J.N. Orce).

https://doi.org/10.1016/j.physletb.2019.03.021

where χ_{M1} is the static magnetic dipole polarizability and considers the sum of the paramagnetic χ_{M1}^{para} and diamagnetic χ_{M1}^{dia} susceptibilities of nuclei [14],

$$\chi_{M1} = \chi_{M1}^{para} + \chi_{M1}^{dia} = 2\sum_{n} \frac{\langle i \parallel \hat{M1} \parallel n\rangle\langle n \parallel \hat{M1} \parallel i\rangle}{E_\gamma} - \frac{Ze^2}{6mc^2}\langle r^2\rangle. \quad (5)$$

According to the independent-particle shell model (IPM), diamagnetism is dominant for nuclei with $A > 60$ [15], but has a negligible effect in σ_{-2} values. Paramagnetism dominates in light nuclei with the rise of permanent magnetic dipole moments and can, in contrast, contribute substantially to σ_{-2} values for nuclei with $A < 20$ [15].

Because of the $1/E_\gamma^2$ energy weighting in Eq. (3), σ_{-2} values are extremely sensitive measures – unlike σ_{total} – of low-energy long-range correlations in the nuclear wave functions, which are common feature for all nucleon-nucleon potentials, and fundamental for shell-model (SM) calculations of heavy nuclei [16] using low-momentum interactions [17]. Intermediate and short-range correlations to the nuclear wave functions from above the GDR region (e.g., nucleon resonances at $E_\gamma \gtrsim 140$ MeV) have a negligible effect on σ_{-2} values [18–21].

Below the neutron separation threshold, the pygmy dipole resonance (PDR) in neutron-rich nuclei [22] – the PDR is an electric dipole resonance arising from the oscillation of a symmetric proton-neutron core against the neutron skin – may add a $\simeq 5\%$ contribution to σ_{-2} values [23]. To a lesser extent, soft resonances such as the $M1$ scissors mode and spin-flip may also contribute. A potentially larger effect to σ_{-2} values may arise from the low-energy enhancement (LEE) of the radiative or photon strength function $f(E_\gamma)$ – indicating the ability of nuclei to emit and absorb photons with energy E_γ – observed at $E_\gamma \lessapprox 4$ MeV [24–26]. This Letter shows how the LEE and GDR cross-section contributions affect σ_{-2} values and may provide evidence for the continuing influence of shell effects at high-excitation energies. Relevant consequences arise from these findings; for instance, the possibility to identify new magic numbers.

The physical origin of the LEE remains ambiguous and its observation seems to be generally associated with weakly deformed nuclei. It has been observed in nearly-spherical nuclei in the $A \approx 50$ and 90 mass regions starting at $E_\gamma \approx 3$–4 MeV. For heavy nuclei, it is only found in ^{105}Cd [27], ^{138,139}La [28] and ^{151,153}Sm [29], where the LEE starts at a lower $E_\gamma \approx 2$ MeV. These findings assume the validity of the Brink-Axel hypothesis – stating that $f(E_\gamma)$ is independent of the particular nuclear structure and only depends on E_γ [30,31] – which has been confirmed experimentally [32,33]. The reason for not being observed in other heavy nuclei – studied with the same experimental method – could relate to the unprecedented sensitivity achieved by Simon and co-workers in ^{151,153}Sm using high-purity germanium (HPGe) detectors in connection with bismuth germanate (BGO) shields [29]. Another relevant finding is that the LEE presents a dominant dipole radiation [26,32], but whether its nature is either electric or magnetic remains unresolved [34]. The recent polarization asymmetry measurements of γ rays in ^{56}Fe using GRETINA tracking detectors yields inconclusive results, although rather suggests an admixture of electric and magnetic dipole radiation, with a small bias towards a magnetic character at $E_\gamma = 1.5$–2.0 MeV [34].

Two competing scenarios are proposed theoretically to explain the LEE anomaly. On one hand, Litvinova and Belov propose that the LEE in $f(E_\gamma)$ occurs because of $E1$ excitations from the hot-quasicontinuum to the continuum region [35]. On the other hand, SM calculations predict that the LEE has a predominant magnetic-dipole $M1$ character. In particular, Schwengner, Frauendorf and Larsen suggest that the LEE arises from active high-j proton and neutron orbits near the Fermi surface with magnetic moments adding up coherently [36]. This is a similar mechanism to the magnetic rotation [37] or two-phonon mixed-symmetry states found in nearly-spherical nuclei at about 3 MeV [38,39]. In a complementary picture, Brown and Larsen suggest that the LEE arises because of the large $M1$ diagonal matrix elements of high-ℓ orbitals [40]. Additionally, Sieja computed both $E1$ and $M1$ strengths in ^{44}Sc on equal footing from large-scale SM calculations and also supported the $M1$ character of the LEE in the $A \sim 50$ region against $E1$ contributions [41,42]. Recently, large-scale SM calculations of neutron-rich ^{70}Ni [43] and many other nuclei [44], using various effective interactions, also support the $M1$ character for the LEE.

Recently, in principle, the validation of these SM predictions in the quasi-continuum region may be arguable as, for instance, they are structure dependent; hence, posing a fundamental question about the validity of the Brink-Axel hypothesis [30,31].

A priori, the comparison of the LEE and the GDR built on ground states is somewhat misleading as the former corresponds to γ-ray transitions between excited states in the quasi-continuum, whereas the latter involves transitions to the ground state. Nonetheless, the study of (p,γ) and (n,γ) reactions for light nuclei and fusion-evaporation reactions for heavy nuclei have shown that GDRs can also be built on excited states (GDR^{exc}) [45–47]. In fact, GDRs^{exc} present – at least for moderate average temperature T and spin J – similar centroid energies, E_{GDR}^{exc}, and resonance strengths, S_{GDR}^{exc}, relative to the Thomas-Reiche-Kuhn (TRK) $E1$ sum rule [48], as those found for the ground-state counterparts (GDR$^{g.s.}$) [45,46]. These similar features suggest a common physical origin for all GDRs in concordance with the Brink-Axel hypothesis, which also indicates that a GDR can be built on every state in a nucleus [30,31]. Moreover, the sum rules in Eqs. (2) and (5) can also be applied to final excited states $|f\rangle$ [49–51]. Henceforth, we assume similar resonance strengths for GDRs built on the ground and excited states. This may explain the nice fit between the high γ-ray energy part of the measured $f(E_\gamma)$ and the left tail of the GDR$^{g.s.}$ (see e.g. [52]).

In order to combine cross-section contributions from the LEE and GDR regions, we use the well-known relation [53],

$$f(E_\gamma) = \frac{1}{g_J \pi^2 (\hbar c)^2} \frac{\sigma_{total}(E_\gamma)}{E_\gamma} \text{ MeV}^{-3}, \quad (6)$$

where $g_J = \frac{2J_f+1}{2J_i+1}$ is the statistical factor, with J_i and J_f being the spins of the initial and final states, respectively. The magnitude of g_J affects the estimation of σ_{-2} values in the LEE region. However, assuming a predominant dipole character for the LEE radiation [26,32,34], a value $g_J = 1$ is valid for $J \rightarrow J$ dipole transitions and a good approximation for any $\Delta J = 1$ spin distribution typically populated (up to $J = 8 - 10\hbar$) in the experimental studies of $f(E_\gamma)$ [54]. This approximation is not valid for GDR $E1$ transitions in even-even nuclei where $g_J = 3$ applies.

The data spanning the GDR region have been obtained from available experimental nuclear reaction data bases, EXFOR [55] and ENDF [56]. Data corresponding to the LEE – in units of MeV^{-3} – have been collected from the Oslo compilation of level densities and $f(E_\gamma)$ [57]. The resulting $\sigma_{total}(E_\gamma)$ was modeled using a cubic-spline interpolation – which assumes validity of the Brink-Axel hypothesis – in order to compute the total cross section and σ_{-2} values. Fourth-order polynomial fits yield similar results to the cubic spline interpolation, with almost negligible differences for the integrated σ_{-2} values of <0.5%. Lower and higher-order interpolation polynomials predict unanticipated structures of the (γ,n) cross-section (e.g. pronounced bumps between the LEE and GDR regions).

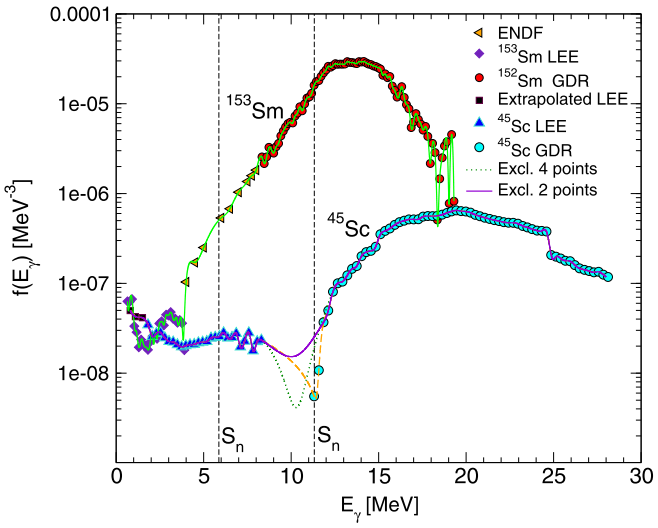

Fig. 1. $f(E_\gamma)$ vs E_γ on a log scale showing the interpolation to the data (solid lines) for ^{45}Sc [58–60] and ^{153}Sm [29,71]. Vertical dash lines indicate the neutron separation energy. See text for additional information.

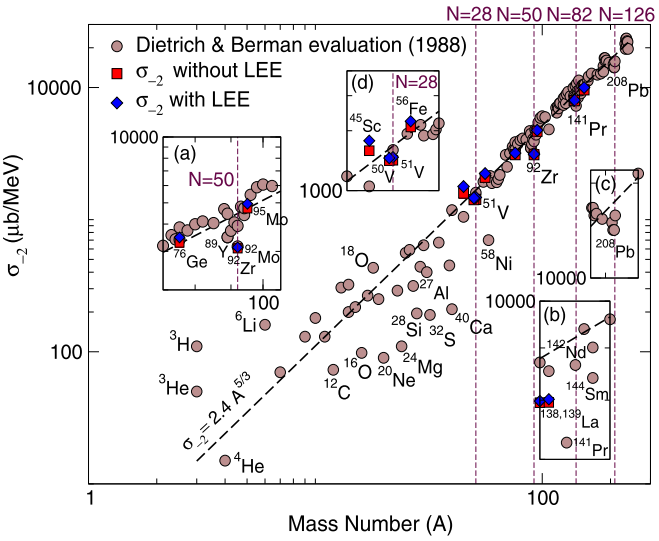

Fig. 2. σ_{-2} *vs* A on a log-log scale from the photo-neutron cross-section evaluation (solid circles) [13] and σ_{-2} data listed in Table 1 excluding (squares) and including (diamonds) the LEE contributions. For comparison, Eq. (7) (dashed line) is plotted.

When available, ENDF data have been utilized to fill the typical gap between the LEE and GDR data sets, as shown in Fig. 1 for the case of ^{153}Sm. Nuclei at different mass regions are evaluated for a systematic study of the LEE and GDR effects on σ_{-2} values. The results are listed in Table 1 and Fig. 1 shows the particular fits to the ^{45}Sc and ^{153}Sm data. Uncertainties on σ_{-2} values arise from the *RMS* deviation, which accounts for a 7% error from the lower and upper loci limits provided by GDR and LEE data [57].

For the particular case of ^{45}Sc, the large E_γ gap between the LEE and GDR data resulted in unrealistic fits with a drastic drop of σ_{-2} values, as shown in Fig. 1. Additional fits were performed by rejecting either the last two or the last four GDR data points at lower E_γ. Fig. 1 shows that the former (solid line) is clearly more realistic and the resulting σ_{-2} value – with a 4% increase with respect to the fit considering the four GDR data points – is quoted in Table 1. Fits to the data for the rest of nuclei studied in this work do not present such large energy gaps and re-fitting of the data was not found necessary.

Although the work by Jones and co-workers supports an increasing trend of LEE for $E_\gamma < 1$ MeV [34], there is little evidence on how $f(E_\gamma)$ behaves approaching $E_\gamma = 0$. Hence, the low-energy cut off has arbitrarily been set to 800 keV for the nuclides considered in this work up to ^{139}La, which incidentally is the typical energy for strong $M1$ isovector transitions in nearly-spherical nuclei [16]. For ^{153}Sm, a low-energy cut off of 645 keV has been set from $f(E_\gamma)$ data [29]. Because of their instability, there is no available GDR information in ^{153}Sm, ^{138}La and ^{50}V, and, instead, GDR data from ^{152}Sm, ^{139}La and ^{51}V, respectively, have been used in the analysis, under the assumption that nearby isotopes present equal $f(E_\gamma)$ (see e.g. [24] and [72]). This assumption may not be adequate given the rapid shape transition from weakly deformed in ^{150}Sm to a well-deformed rotor in ^{154}Sm, and the realization of shell closures in ^{139}La ($N = 82$) and ^{51}V ($N = 28$).

For comparison, Fig. 2 shows overall σ_{-2} values of ground states as a function of A extracted from photo-neutron cross sections using monoenergetic photon beams and determined above neutron threshold to an upper limit of $E_{\gamma max} \approx 20$–50 MeV [13]. The data include the GDR region and are representative for nuclei above $A \gtrsim 50$ (except for ^{58}Ni [73]), where neutron emission is generally the predominant decay mode. This may not be true for nuclei with semi-magic number of neutrons – discussed below – where proton separation energies may lie lower than neutron thresholds.

From Eqs. (1) and (2), Migdal extracted the relation $\sigma_{-2} = 2.25A^{5/3}$ μb/MeV, which was qualitatively confirmed by Levinger [21] and further refined [74] as (dashed line in Fig. 2),

$$\sigma_{-2} = 2.4(1)\kappa\ A^{5/3}\ \mu\text{b/MeV}, \tag{7}$$

Table 1
Contributions of GDR and LEE cross-sections to σ_{-2} and κ values. Data have been extracted from EXFOR [55], ENDF [56] and the Oslo compilation [57]. An asterisk indicates that the σ_{-2} value includes $\sigma(\gamma, p)$ contributions.

Nucleus	$E_{\gamma(max)}$(GDR) (MeV)	$E_{\gamma(max)}$(LEE) (MeV)	σ_{-2}(total) (μb/MeV)	σ_{-2} (LEE)	κ (LEE)	[Refs.]
$^{45}_{21}$Sc*	28.1	3.2	1840(130)	9.7%	1.35(9)	[58–60]
$^{50}_{23}$V	27.8	3.1	1458(100)	2.9%	0.89(7)	[52,61]
$^{51}_{23}$V	27.8	3.1	1472(100)	3.3%	0.87(7)	[52,61]
$^{56}_{26}$Fe*	40.0	3.8	2231(155)	6.3%	1.13(8)	[26,62]
$^{76}_{32}$Ge	26.5	2.3	3189(225)	2.7%	0.97(7)	[63,64]
$^{92}_{40}$Zr	27.8	2.2	3131(220)	1.1%	0.70(5)	[65–67]
$^{95}_{42}$Mo	27.8	2.5	4743(330)	1.7%	1.00(7)	[68,69]
$^{138}_{57}$La	24.3	1.9	7983(560)	0.4%	0.90(7)	[28,70]
$^{139}_{57}$La	24.3	2.5	8015(560)	0.7%	0.90(6)	[28,70]
$^{153}_{62}$Sm	20.0	1.6	9999(700)	2.7%	0.95(7)	[29,71]

where κ is the polarizability parameter and represents deviations from the actual GDR effects. This result is in excellent agreement with IPM predictions using, instead of $\hbar\omega = 41A^{-1/3}$ MeV, $E_{GDR}^{g.s.} = 79A^{-1/3}$ MeV as the resonance frequency [75]. A value of $\kappa = 1$ generally holds for the ground state of nuclei with $A \gtrapprox 50$, and probably for even lighter nuclei with $A \gtrapprox 20$ once $\sigma(\gamma, p)$ contributions are taken into account [21,73,74]. In contrast, values of $\kappa > 1$ are generally found for light nuclei with $A < 20$ [21, 49–51,74,76,77], where paramagnetism is important.

Sudden drops of σ_{-2} (and κ) values are apparent for the $N = 50$, 82 and 126 isotones in the insets (a), (b) and (c) of Fig. 2, respectively. Above both proton and neutron separation energies, the photo-absorption cross section in the lower energy part of the GDR is controlled by the statistical competition between $\sigma(\gamma, p)$ and $\sigma(\gamma, n)$ contributions, which presents a strong correlation with the level density ratio N_p/N_n between the open neutron (N_n) and proton (N_p) channels [73], $\sigma(\gamma, p)/\sigma(\gamma, n) \approx N_p/N_n$. This ratio depends on the neutron and proton penetrabilities, ϵ_n and ϵ_p, respectively, as more energy is needed for protons to overcome the Coulomb barrier.

Total photo-absorption cross-sections ($\sigma(\gamma, n) + \sigma(\gamma, p)$) are reasonably available in the $N = 50$ isotones, with the latter being indirectly determined from $(e, e'p)$ measurements [60]. The $\sigma(\gamma, p)$ contribution is particularly important for ^{92}Mo, with $N_p/N_n \approx 1.95$, and decreases for the lighter $N = 50$ isotones, with $N_p/N_n \approx 0.66, < 0.28$ and 0.09 for ^{90}Zr, ^{89}Y and ^{88}Sr, respectively [68], as the isospin quantum number $T_z = \frac{N-Z}{2}$ increases. The $\sigma(\gamma, p)$ contribution extracted from the N_p/N_n ratio only applies to the lower energy half of the GDR, and $\sigma(\gamma, n)$ contributions still remain greater. Once $\sigma(\gamma, p)$ contributions are taken into account, the total photo-absorption cross section satisfies the TRK sum rule [68], $\frac{\sigma_{total}(\gamma,n)+\sigma_{total}(\gamma,p)}{0.06NZA^{-1}}$. For the ^{92}Mo case, there remains $\approx 35\%$ $\sigma(\gamma, p)$ contribution to the total photo-absorption cross section [60], which explains the sharper drop in the σ_{-2} value shown in Fig. 2(a). More conspicuous are the drops of σ_{-2} values in ^{89}Y, ^{141}Pr and ^{208}Pb – where $\sigma(\gamma, n)$ contributions strongly dominate – which could provide evidence for shell effects. Clearly, direct measurements of $\sigma(\gamma, p)$ contributions are crucially needed for singly- and doubly-magic nuclei.

Furthermore, Table 1 shows that the LEE has a substantial contribution to σ_{-2} values in medium-mass nuclei (^{45}Sc and ^{56}Fe) away from the $N = 28$ shell closure, being largest for ^{45}Sc with $\approx 10\%$ increase. As illustrated in Fig. 1, this enhancement partly arises because of the inverse mass dependence of E_{GDR} and the fact that the LEE starts at lower E_γ as A increases. In fact, Table 1 shows that the LEE has a negligible contribution of $\lesssim 3\%$ to the total σ_{-2} values of heavy nuclei with $A \gtrsim 76$. A stronger contribution to σ_{-2} values would arise if the LEE trend keeps increasing at energies approaching $E_\gamma = 0$, as predicted by SM calculations. This possibility will be explored in detail in a separate manuscript [78].

More intriguing are the small overall contributions to σ_{-2} values found in nuclei close to or having a magic number. When compared with Eq. (7), these nuclides present evident deviations from GDR effects (i.e. $\kappa \neq 1$) with smaller values of $\kappa \approx 0.90$ in ^{50,51}V ($N \approx 28$) and ^{138,139}La ($N \approx 82$), and specially for ^{92}Zr ($N \approx 50$ and $Z = 40$) with $\kappa = 0.70(5)$. In contrast, heavy nuclei away from shell closures present polarizability parameters consistent with $\kappa = 1$; except perhaps for ^{153}Sm, where we used the ^{152}Sm data for the GDR region and a cut-off of $E_\gamma = 645$ keV. This recurrent behavior to the one previously observed in the photoneutron cross-section data for the $N = 50$, 82 and 126 isotones, indicates the continuing influence of shell effects in the quasi-continuum region up to the neutron threshold. As shown in Table 1 and inset (d) in Fig. 2, this is consistent with the smaller LEE contribution to the total σ_{-2} values of ^{50,51}V ($N \approx 28$) with respect to the neighboring ^{45}Sc and ^{56}Fe nuclides. Although there is no $\sigma(\gamma, p)$ data available for ^{50,51}V, (γ, p) contributions will relatively be much weaker for ^{51}V because of the much lower level density of the open proton channel (even-even ^{50}Ti with $N = 28$) as compared with the open neutron channel (odd-odd ^{50}V).

Interesting SM calculations of the $M1$ strength in the LEE for various isotopic and isotonic chains by Midtbo and collaborators [44] predict a relatively sharper increase of the $M1$ strength at $E_\gamma = 0$–2 MeV for neutron-rich nuclei when approaching shell closure. These results may contradict our findings for stable nuclei and suggest the enhancement of nuclear polarizability with increasing instability.

Conclusively, drops of σ_{-2} values ($\kappa < 1$) for several nuclei with, or close to, neutron magic numbers $N = 28$, 50, 82 and 126, suggest that the shell model remains valid at high excitation energies, from the quasi-continuum to the GDR region; in agreement with Balashov's SM interpretation of the GDR as a system of independent nucleons plus the residual interaction [79]. These deviations from GDR effects, because of the nature of Eq. (7), are plausibly not related to $E1$ transitions, which, together with the continuing influence of shell effects, strongly support the $M1$ interpretation of the LEE by large-scale SM calculations [36,40–43]. Moreover, the empirical evidence for shell effects suggests that the generalized Brink-Axel hypothesis allows for structural changes and is, therefore, more universal than originally expected. This conclusion is supported by the work of Larsen et al. [32], where $f(E_\gamma)$ trends are found to be preserved for different bin energies.

Finally, we confirm the induction of permanent magnetic dipole moments or paramagnetism in the quasi-continuum region, in agreement with previous SM calculations and IPM predictions of an enhanced paramagnetism for the ground states of nuclei with large occupation number of the shells determining the magnetic properties [14]. The origin of this paramagnetism can be inferred from SM calculations, which can distinguish between single-particle spin-flips and collective isovector excitations by decomposing the relevant $M1$ strength into their spin and orbital components [16]. Similar to two-neutron separation energies extracted from atomic mass measurements of ground and isomeric states, this work opens a new research avenue to investigate the evolution of shell closures and the existence of "old" and "new" magic numbers at high-excitation energies from σ_{-2} measurements.

Acknowledgements

The authors acknowledge Physics discussions with B. Dey, P.E. Garrett, B.V. Kheswa, A. Pastore, S. Triambak, K. Sieja, P. von Neumann-Cosel and M. Wiedeking. This work was supported by the National Research Foundation of South Africa under Grant 93500, the SA-CERN Collaboration and the MaNuS/MatSci Honours/Masters program.

References

[1] A. Migdal, J. Exp. Theor. Phys. USSR 15 (1945) 81.
[2] C.F. von Weizsäcker, Z. Phys. 96 (1935) 431.
[3] H.A. Bethe, R.F. Bacher, Rev. Mod. Phys. 8 (1936) 82.
[4] H. Steinwedel, J.H.D. Jensen, P. Jensen, Phys. Rev. 79 (1950) 1019.
[5] G.C. Baldwin, G.S. Klaiber, Phys. Rev. 71 (1947) 3.
[6] J.P. Connerade, J.M. Esteva, R.C. Karnatak, Giant Resonances in Atoms, Molecules and Solids, NATO ASI Ser., Ser. B: Phys., vol. 151, 1986.
[7] M. Jablan, M. Soljačić, H. Buljan, Proc. IEEE 101 (2013) 1689.
[8] O. Bohigas, N. van Giai, D. Vautherin, Phys. Lett. B 102 (1981) 105.
[9] Z. Zhang, Y. Lim, J.W. Holt, C.M. Ko, Phys. Lett. B 777 (2018) 73.
[10] D. Gambacurta, M. Grasso, O. Vasseur, Phys. Lett. B 777 (2018) 163.
[11] J.S. Levinger, Nuclear Photo-Disintegration, Oxford University Press, Oxford, 1960.
[12] A.B. Migdal, A.A. Lushnikov, D.F. Zaretsky, Nucl. Phys. A 66 (1965) 193.
[13] S.S. Dietrich, B.L. Berman, At. Data Nucl. Data Tables 38 (1988) 199.

[14] W. Knüpfer, A. Richter, Z. Phys. A 320 (1985) 253.
[15] W. Knüpfer, A. Richter, Phys. Lett. B 107 (1981) 325.
[16] J.N. Orce, et al., Phys. Rev. Lett. 97 (2006) 062504.
[17] S.K. Bogner, R.J. Furnstahl, A. Schwenk, Prog. Part. Nucl. Phys. 65 (2010) 94.
[18] L.W. Jones, K.M. Terwilliger, Phys. Rev. 91 (1953) 699.
[19] D.W. Kerst, G.A. Price, Phys. Rev. 79 (1950) 725.
[20] J. Ahrens, H. Gimm, A. Zieger, B. Ziegler, Nuovo Cimento A 32 (3) (1976) 364.
[21] J.S. Levinger, Phys. Rev. 107 (1957) 554.
[22] N. Paar, D. Vretenar, E. Khan, G. Colo, Rep. Prog. Phys. 70 (2007) 691.
[23] P. von Neumann-Cosel, Phys. Rev. C 93 (2016) 049801.
[24] M. Guttormsen, et al., Phys. Rev. C 71 (2005) 044307.
[25] M. Wiedeking, et al., Phys. Rev. Lett. 108 (2012) 162503.
[26] A.C. Larsen, et al., Phys. Rev. Lett. 111 (2013) 242504.
[27] A.C. Larsen, et al., Phys. Rev. C 87 (2013) 014319.
[28] B.V. Kheswa, et al., Phys. Lett. B 744 (2015) 268.
[29] A. Simon, et al., Phys. Rev. C 93 (2016) 034303.
[30] D. Brink, doctoral thesis, Oxford University, 1955 (unpublished).
[31] P. Axel, Phys. Rev. 126 (1962) 671.
[32] A.C. Larsen, et al., J. Phys. G 44 (2017) 064005.
[33] M. Guttormsen, et al., Phys. Rev. Lett. 116 (2016) 012502.
[34] M.D. Jones, et al., Phys. Rev. C 97 (2018) 024327.
[35] E. Litvinova, N. Belov, Phys. Rev. C 88 (2013) 031302(R).
[36] R. Schwengner, S. Frauendorf, A.C. Larsen, Phys. Rev. Lett. 111 (2013) 232504.
[37] R. Schwengner, et al., Phys. Rev. C 66 (2002) 024310.
[38] N. Pietralla, et al., Phys. Rev. Lett. 83 (1999) 1303.
[39] C. Fransen, et al., Phys. Rev. C 67 (2003) 024307.
[40] B.A. Brown, A.C. Larsen, Phys. Rev. Lett. 113 (2014) 252502.
[41] K. Sieja, Phys. Rev. Lett. 119 (2017) 052502.
[42] K. Sieja, EPJ Web Conf. 146 (2017) 05004.
[43] A.C. Larsen, et al., Phys. Rev. C 97 (2018) 054329.
[44] J.E. Midtbø, A.C. Larsen, T. Renstrøm, F.L. Bello Garrote, E. Lima, Phys. Rev. C 98 (2018) 064321.
[45] J.J. Gaardhøje, Annu. Rev. Nucl. Part. Sci. 42 (1992) 483.
[46] K.A. Snover, Annu. Rev. Nucl. Part. Sci. 36 (1986) 545.
[47] A. Schiller, M. Thoennessen, At. Data Nucl. Data Tables 93 (2007) 549.
[48] J.S. Levinger, H.A. Bethe, Phys. Rev. 78 (1950) 115.
[49] O. Häusser, et al., Nucl. Phys. A 212 (1973) 613.
[50] J.N. Orce, et al., Phys. Rev. C 86 (2012) 041303(R).
[51] M.K. Raju, et al., Phys. Lett. B 777 (2018) 250.
[52] A.C. Larsen, et al., Phys. Rev. C 73 (2006) 064301.
[53] G.A. Bartholomew, et al., Adv. Nucl. Phys. 7 (1973) 229.
[54] V.B. Kheswa, private communication.
[55] https://www-nds.iaea.org/exfor/exfor.htm.
[56] https://www.nndc.bnl.gov/ensdf/.
[57] http://www.mn.uio.no/fysikk/english/research/about/infrastructure/OCL/nuclear-physics-research/compilation/.
[58] A. Vessiere, et al., Nucl. Phys. A 227 (1974) 513.
[59] A.C. Larsen, et al., Phys. Rev. C 76 (2007) 044303.
[60] K. Shoda, Nucl. Phys. A 239 (1975) 397.
[61] S.C. Fultz, et al., Phys. Rev. 128 (1962) 2345.
[62] S.S. Borodina, et al., Moscow State Univ. Inst. of Nucl. Phys. Rep. (2000) 6.
[63] P. Carlos, et al., Nucl. Phys. A 258 (1976) 365.
[64] A. Spyrou, et al., Phys. Rev. Lett. 113 (2014) 232502.
[65] B.L. Berman, et al., Phys. Rev. 162 (1967) 1098.
[66] M. Guttormsen, et al., Phys. Rev. C 96 (2017) 024313.
[67] H. Utsunomiya, et al., Phys. Rev. Lett. 100 (2008) 162502.
[68] H. Beil, et al., Nucl. Phys. A 227 (1974) 427.
[69] H. Utsunomiya, et al., Phys. Rev. C 88 (2013) 015805.
[70] H. Beil, et al., Nucl. Phys. A 172 (1971) 426.
[71] P. Carlos, et al., Nucl. Phys. A 225 (1974) 171.
[72] M. Guttormsen, et al., Phys. Rev. C 68 (2003) 064306.
[73] R. Bergère, Lect. Notes Phys. 61 (1977) 1.
[74] J.N. Orce, Phys. Rev. C 91 (2015) 064602.
[75] O. Bohigas, Lect. Notes Phys. 137 (1981) 65.
[76] W.J. Vermeer, et al., Aust. J. Phys. 35 (1982) 283.
[77] F.C. Barker, Aust. J. Phys. 35 (1982) 291.
[78] C. Ngwetsheni, J.N. Orce, submitted to Hyperfine Interactions, 2019.
[79] V.V. Balashov, J. Exp. Theor. Phys. USSR 42 (1962) 275.